

High temperature structural and magnetic properties of cobalt nanorods.

Kahina Ait Atmane^a, Fatih Zighem^b, Yaghoub Soumare^a, Mona Ibrahim^c, Rym Boubekri^c, Thomas Maurer^b, Jérémie Margueritat^b, Jean-Yves Piquemal^a, Frédéric Ott^b, Grégory Chaboussant^b, Frédéric Schoenstein^d Noureddine Jouini^d and Guillaume Viau^c
^a*ITODYS, CNRS/Université Paris Diderot, Sorbonne Paris Cité, 75205 Paris, France*
^b*LLB, CEA/CNRS, IRAMIS, 91191 Gif sur Yvette, France*
^c*LPCNO, CNRS/INSA-Université de Toulouse, 31077 Toulouse, France and*
^d*LSPM, CNRS/Université Paris XIII, 93430 Villetaneuse, France**

I. INTRODUCTION

The last decade has seen numerous investigations on anisotropic inorganic nanoparticles such as nanowires (NWs) and nanorods (NRs) for their peculiar physical properties and new applications in optics, magnetism or electronics [1, 2]. Several physical and chemical methods have been developed to grow ferromagnetic nanowires. The most used consists in the electrochemical reduction of Fe, Co or Ni salts within the uniaxial pores of an alumina or a polycarbonate membrane to confine the metal growth [3]. In order to grow NWs with a diameter below 10 nm, other solid hosts have been employed such as carbon nanotubes [4] or mesoporous silica [5]. Recently, cobalt NWs with diameters below 5 nm embedded in epitaxial CeO₂ layers were obtained by pulsed-laser deposition [6]. Iron-boride NWs with diameter in the range 5-50 nm were obtained by chemical vapour deposition [7]. Wet chemistry methods, for which the adsorption of long chain molecules at the metal particle surface is the driving force of the anisotropic growth, were developed for the synthesis of cobalt [8] and cobalt-nickel NRs and NWs [9].

One interest of high aspect ratio ferromagnetic nanoparticles is that they can present high coercivity properties due to their large shape anisotropy. Magnetic NWs have been recently proposed as potential candidates for high-density magnetic recording [10, 11], nanowire-based motors [11] and the bottom-up fabrication of permanent magnets [12]. Indeed, very high coercivity values were observed on assemblies of cobalt NRs or NWs obtained using wet chemistry, either by the polyol process [13] or by organometallic chemistry [14]. Composite materials of well aligned cobalt rods with a volume fraction of 50% could exhibit higher (BH)_{max} values than AlNiCo or ferrite-based magnets [11]. The interest of these liquid phase processes for the synthesis of NRs with hard magnetic properties lies in the possibility to produce wires combining very good crystallinity and small diameter. The cobalt NRs and NWs synthesized by these chemical methods crystallize with a hcp

structure with the c axis along the long axis [8, 15]. The coincidence of the shape anisotropy easy axis and the magneto-crystalline anisotropy easy axis reinforces the whole magnetic anisotropy [12, 14].

Several parameters govern the coercivity of an assembly of anisotropic magnetic particles: (i) the distribution of the particle easy axis orientation with respect to the magnetic field and (ii) the particles shapes. For cobalt wires we showed that the coercivity increases when they are aligned parallel to the applied magnetic field in good agreement with the Stoner-Wohlfarth model [13]. The coercivity is the sum of the magnetocrystalline and the anisotropy contributions. The contribution due to the shape anisotropy actually strongly depends on the detailed geometry of the wires and especially of the wire tips. This was investigated by micro-magnetic simulations [16]. On the one hand, while the ellipsoid shape is the most favourable, a cylindrical shape also provide a good shape anisotropy. On the other hand, enlarged tips create nucleation points for the magnetization reversal which can significantly reduce the coercivity by up to 30. Surface effects related to the thin superficial CoO layer were extensively studied [18]. The measured Néel temperature of the CoO shell was 230 K. Significant modifications of the magnetic behaviour take place below this temperature. When the temperature decreases, a coercivity drop is actually observed below 150 K [18].

But even if progresses have been made in the synthesis of ferromagnetic NRs and NWs exhibiting large coercivities at room temperature and in the understanding of their magnetic properties [12, 13, 16–18], there is still a lack of information about the stability of both their structural and magnetic properties above room temperature which is a key information for any practical use at high temperatures of these materials e.g. for the fabrication of rare-earth free permanent magnets. At high temperatures, metal wires generally undergo an irreversible transformation to chains of spheres, described as the Rayleigh instability [19, 20]. The high aspect ratio of compacted wires may also be altered by sintering. A first study showed that the thermal stability of “organometallic” cobalt nanowires was dependent on the atmosphere under which the wires were annealed [21]. Fragmentation of cobalt NWs into chains of cobalt particles due to the Rayleigh instability was avoided

*Electronic address: jean-yves.piquemal@univ-paris-diderot.fr (J.-Y.P.); gviau@insa-toulouse.fr (G.V.)

when the cobalt NWs were coated by a thin carbon shell [21].

In this paper we present the high temperature structural and magnetic properties of cobalt nanorods prepared by the polyol process using in-situ characterizations. The scope of this communication is to determine whether the anisotropic structure and texture are modified at high temperature and consequently whether their magnetic properties, and especially their large coercivities, are preserved. The temperature range of stability of these NRs and the temperature dependence of their intrinsic magnetic properties up to 623 K under different atmospheres are described.

II. MATERIALS AND METHODS.

$\text{CoCl}_2 \cdot 6\text{H}_2\text{O}$ (Alfa Aesar, 99.9%), $\text{RuCl}_3 \cdot x\text{H}_2\text{O}$ (Aldrich, 99.98%), NaOH (Acros), 1,2- butanediol (Fluka, $\geq 98\%$), methanol (VWR, Normapur) and sodium laurate, $\text{Na}(\text{C}_{11}\text{H}_{23}\text{COO})$ (Acros, 98%) were used without any further purification.

A. Syntheses of Co nanowires.

The cobalt laurate precursor, $\text{Co}^{\text{II}}(\text{C}_{11}\text{H}_{23}\text{COO})_2$ was first prepared. In 100 mL of distilled water at 333 K, was dissolved sodium laurate (75 mmol; 16.7 g) and to this solution, was added an aqueous solution (38 mL) of cobalt(II) chloride (40 mmol, 10.0 g) pre-heated at 333K under vigorous stirring. This resulted in the formation of a purple precipitate which was vigorously stirred at 333K for 15 min. The Co(II) solid phase was washed twice with distilled water (100 mL) then with methanol (100 mL) and finally dried in an oven at 323 K overnight. Yield: 94% (based on Co).

The synthesis of the cobalt NRs was realized according to a procedure previously described [13]. To 75.0 mL of 1,2-butanediol were added $\text{Co}(\text{C}_{11}\text{H}_{23}\text{COO})_2$ (2.75 g, 0.08 M), $\text{RuCl}_3 \cdot x\text{H}_2\text{O}$ ($3.2 \cdot 10^{-2}$ g) and NaOH (0.225 g, 0.075 M). The mixture was heated to 448 K with a ramping rate of $13 \text{ K} \cdot \text{min}^{-1}$ for 20 min until the color of the solution turned black, indicating the reduction of Co(II) into metallic cobalt. After cooling to room temperature, the Co NRs were recovered by centrifugation at 8500 r.p.m. for 15 min, washed with 50 mL of absolute ethanol (3 times), and finally dried in an oven at 323 K. Yield: 92% (based on Co). Elemental analyses revealed C and H amounts of 3.8 and 0.7 wt. %, respectively.

B. Preparation of the sample for magnetic measurements.

Two sets of samples were prepared for magnetic measurements. Sample (A): a few drops of a Co NRs sus-

pension in toluene were deposited on an aluminum foil and the toluene was removed by evaporation under the application of an external magnetic field of 1 T. Sample (B): a pellet of magnetic NRs was prepared using an infrared KBr die (internal diameter 13 mm) and applying a pressure of about 6 tons delivered by a hydraulic press. The mass and the apparent density (including porosity) of the pellet were respectively 0.26 g and 2.13 g cm^{-3} . The true density of the powder, obtained at 298 K using a helium Accupyc 1330 pycnometer from Micromeritics, was found to be $6.76 \pm 0.41 \text{ g cm}^{-3}$. The packing factor, defined as the ratio of the volume of the particles by the volume of the pellet was about 30%. Co nanowires are randomly oriented inside the pellet since no magnetic field was applied during its preparation. The small density of the powder is accounted for by the fact that part of the metallic wires are oxidized and that some organic material remain in the pellets.

C. Characterization techniques.

1. Room temperature characterizations

Transmission electron microscopy (TEM) characterizations were performed using a Jeol 100-CX II microscope operating at 100 kV. Infrared spectra were recorded on a nitrogen purged Nicolet 6700 FT-IR spectrometer equipped with a VariGATR accessory (Harrick Scientific Products Inc., NY) fixing the incident angle at 62° . A drop of the colloidal solution was deposited on the Ge wafer and the spectrum was recorded when the solvent (absolute ethanol or toluene) was fully evaporated. XRD patterns obtained using Co K radiation ($\lambda = 1.7889$ Å) were recorded on a PANalytical X'Pert Pro diffractometer equipped with an X'celerator detector in the range $20 - 80^\circ$ with a 0.067° step size and 150 s per step. The size of coherent diffraction domains, L_{hkl} , were determined using MAUD software which is based on the Rietveld method combined with Fourier analysis, well adapted for broadened diffraction peaks. Magnetic measurements were performed using a Quantum Design MPMS-5S SQUID magnetometer.

2. Thermal treatments and high temperature characterizations.

In order to follow the structural evolution of the cobalt nanowires with temperature, insitu thermal treatments were realized in the range 300-673 K, using a HTK 1200N high-temperature X-ray diffraction chamber from Anton Paar. Two types of experiments were performed, depending on the oxygen content of the nitrogen gas used: in the first one, the powder was heated under a high-purity nitrogen atmosphere ($\text{O}_2 < 2 \text{ ppm}$; N_2 Alphagaz 1) while in the second one, the oxygen content was substantially higher ($\text{O}_2 < 0.1 \text{ ppm}$; N_2 Alphagaz 2). The samples

were heated inside the high temperature X-ray diffraction chamber from room temperature to the final temperature using a $5 \text{ K} \cdot \text{min}^{-1}$ rate and maintained for 2 h at the final temperature before the acquisition of a X-ray diffraction pattern. Magnetization curves at high temperature of samples (A) and (B) were measured with a SQUID equipped with an oven. In this procedure the particles were heated in a reduced helium pressure.

III. RESULTS AND DISCUSSIONS

A. Morphology and chemical analysis of the cobalt nanorods.

TEM observations on the particles prepared by the polyol process showed Co NRs with a mean diameter $d_m = 13 \text{ nm}$ and a mean length $L_m = 130 \text{ nm}$ (Figure 1a). The standard deviation of the diameter is very small ($< 15\%$ of the mean length) as it was observed before [13]. For the Co NRs deposited on an Al substrate, the application of an external magnetic field results in the alignment of the cobalt anisotropic nanoparticles while the Co NRs are randomly oriented within the pellet (see Figure 1b and 1c). Moreover Figure 1c shows also that the compression was not detrimental to the Co NRs. The Co NRs were further characterized using TG-DT analyses under pure N_2 ($\text{O}_2 < 0.1 \text{ ppm}$). The thermogram (see Figure 2) showed a 7% weight loss at about 575 K associated with a sharp endothermic peak. This weight loss is attributed to the elimination of organic matter adsorbed on the particle surface. Infrared spectroscopy was thus performed on the cobalt particles to characterize the organic matter remaining after the synthesis and the washing procedure at room temperature. The cobalt NRs infrared spectrum washed twice with ethanol (Figure 3) exhibits a large band centered at 3300 cm^{-1} corresponding to the O-H stretching vibration. The OH groups can belong to a surface cobalt hydroxide and/or to adsorbed ethanol. At 2850 and 2920 cm^{-1} the symmetric and asymmetric C-H stretching vibration are respectively observed, which is attributed to the CH_2 groups of the laurate ions. In the region between 1400 and 1550 cm^{-1} the intense bands are attributed to the asymmetric and symmetric C-O stretching vibration of carboxylate groups, indicating that laurate ions remain at the particle surface. The intensity of all these bands decreases with the successive washings (Figure 3) showing that the amount of organic ligands at the particle surface is strongly dependent on the way they have been washed.

B. High temperature structural and chemical modification.

In order to follow the structural modifications of the Co NRs when they are heated up, in-situ X-ray diffraction

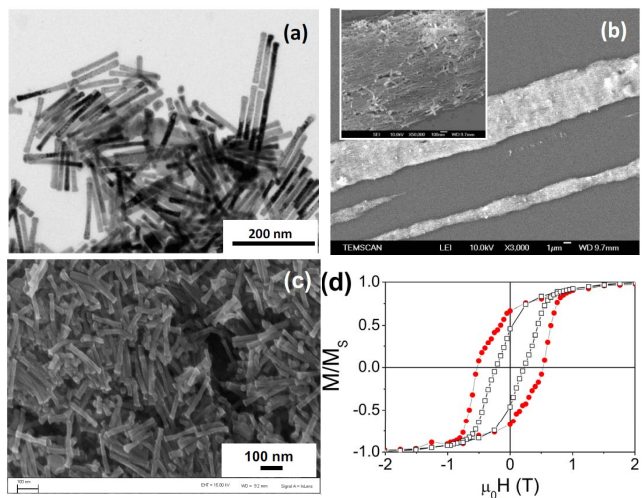


Figure 1: (a) TEM images of Co rods ($L_m = 130 \text{ nm}$, $d_m = 13 \text{ nm}$); SEM images of (b) sample (A), (c) sample (B) and (d) magnetization curves at 300 K of sample (A) (circles) and (B) (squares).

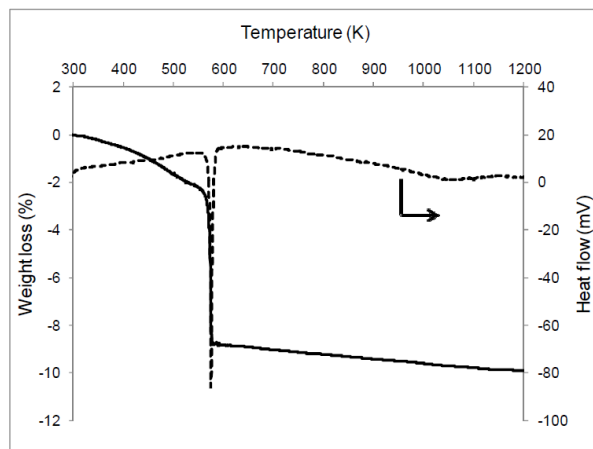


Figure 2: Thermogravimetric and differential thermal analyses realized on Co nanowires under N_2 ($\text{O}_2 < 0.1 \text{ ppm}$).

have been performed for different temperatures ranging from 298 K up to 623 K. The structural and chemical modifications were found to depend on the atmosphere under which the cobalt wires are annealed. The in-situ X-ray diffraction patterns of the Co NRs annealed under a N_2 atmosphere with O_2 concentration $< 2 \text{ ppm}$ at different temperatures showed a progressive oxidation emphasized by the growth of the CoO (111) peak around 42° in spite of the small O_2 concentration. With increasing temperature, the very broad peaks of the oxide becomes thinner indicating grain growth processes and/or crystallization of a pre-existing amorphous phase. Previous HRTEM studies performed on Co nanowires have evidenced the presence of a CoO layer composed of disoriented crystallites of various sizes [18], indicating that

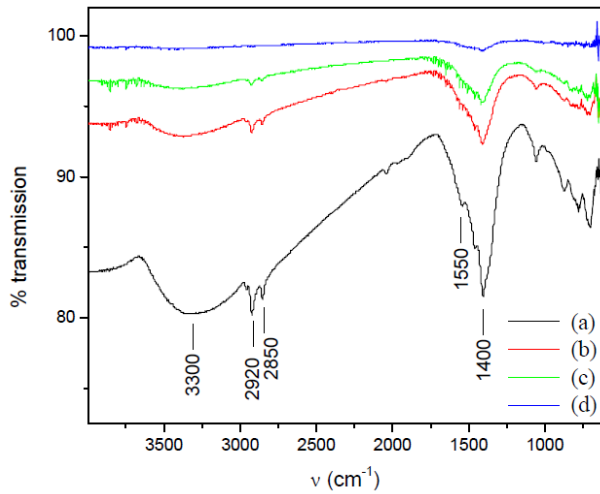


Figure 3: Infrared absorption spectra of cobalt wires washed twice with ethanol (a); washed twice with ethanol and once (b), twice (c) and three times (d) with toluene.

the former case is the more probable one. No structural modification was observed on the hcp non oxidized cobalt phase. For Co samples treated under N_2 with very low dioxygen content (< 0.1 ppm) the Xray diffraction data (Fig. 4) show that there is also development of the CoO oxide between 298K and 473 K. Then, between 473 and 523 K, CoO vanished at the benefit of metallic Co as indicated by the sharpening and the increase of intensity of the Co peaks. For higher temperatures, 573 K and 623 K, CoO is detected again. Given the high temperature applied, the very low dioxygen content is nevertheless sufficient to induce the formation of this oxide. For the as-synthesized sample, TG-DT analyses realized under N_2 (O_2 content < 0.1 ppm) have shown a weight loss of about 7 % at 573 K associated with an endothermic signal (see Figure 2). This weight loss is explained by the decomposition of the remaining metal-organic species adsorbed at the particle surface. Indeed, IR-ATR experiments (Figure 3) have clearly shown vibrations attributed to adsorbed laurate species (see above). Thus, the comparison of the HT XRD patterns with the IR and TGA results suggest that the organic molecules remaining at the particle surface reduce the CoO shell in the temperature range corresponding to their decomposition. This effect can be evidenced only when the oxygen concentration in the atmosphere is small enough.

C. High temperature texture modification.

The XRD diffractograms showed that the hexagonal close-packed structure of the Co core is preserved for temperatures up to 623 K, whatever the annealing atmosphere. Nevertheless, a close examination of these patterns shows that the line broadening is modified during the thermal treatment. The mean crystallite sizes

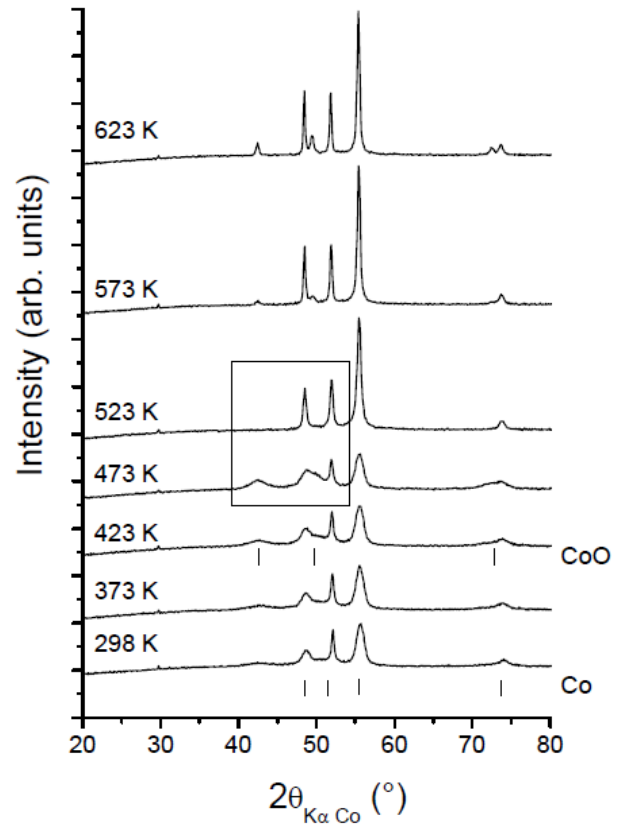


Figure 4: In-situ X-ray diffraction patterns of Co nanorods thermally treated under N_2 ($O_2 < 0.1$ ppm).

for the (10.0) and (00.2) reflexions have been determined and plotted as a function of the temperature treatment for samples annealed in N_2 with the lowest oxygen content (Figure 5). At room temperature, the mean crystallite size for the (10.0) reflexion is always found much smaller than the mean crystallite size for the (00.2) reflexion. This observation confirms that the long axis of the cobalt wires is the c axis of the hcp structure. The data show that up to 500 K, the (10.0) and (00.2) mean crystallite sizes are more or less constant, indicating that the anisotropic shape of the crystallites is preserved. Major texture modifications are observed above 525K. Indeed, at this temperature a considerable increasing of both the $L_{10.0}$ and $L_{00.2}$ mean crystallite sizes is observed and the crystallites lose their anisotropy. At 525 K particles start to undergo sintering. In order to probe a possible deterioration of the Co nanowire morphology, TEM was performed ex-situ for samples annealed at different temperatures. Figures 6a and 6b indicate that the shape of the nanowires is kept up to 523 K. On the other hand, Figure 6c shows that at 573 K and above, the nanowires start to sinter so that their shape anisotropy starts to fade away at these temperatures. At 623 K, the anisotropic shape is lost and only large aggregates are observed (Figure 6d). The sintering of the particles is probably enhanced by the fact that the CoO layer which likely acts as a pro-

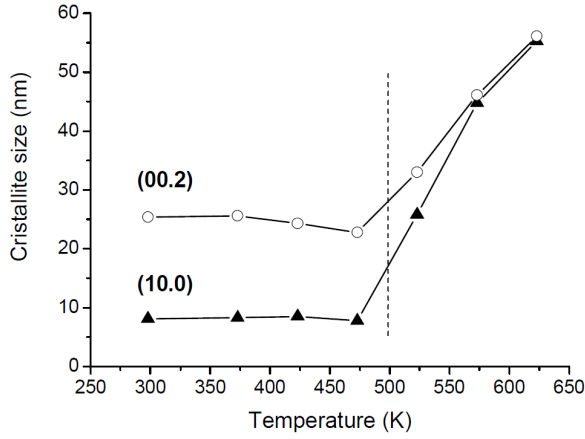


Figure 5: Variation of the $L_{10.0}$ and $L_{00.2}$ mean crystallite sizes with increasing temperature for Co samples treated under N_2 ($O_2 < 0.1$ ppm).

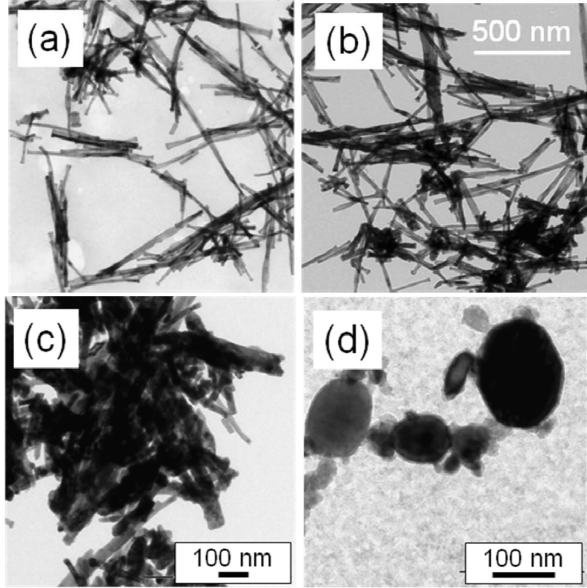


Figure 6: TEM images of Co wires (a) after drying at 330 K and after thermal treatment under N_2 ($O_2 < 0.1$ ppm) for 2 hours at 523 K (b), at 573 K (c) and 2 hours at 623 K (d).

protective layer preventing sintering is reduced to cobalt by the organic molecules at about 523 K as seen by XRD (Figure 4).

D. Magnetic properties at high temperature.

The cobalt NRs are ferromagnetic at room temperature with coercivities of 530 and 230 mT and M_r/M_s values of 0.67 and 0.46 for the samples (A) and (B), respectively. The difference of H_C and M_r are essentially due to the high degree of orientation of the rods in the

sample (A) which increases both coercivity and remanence. The saturation magnetization M_S of sample (B) is 113 emu.g^{-1} ($1.410^{-4} \text{ T.m}^3.\text{kg}^{-1}$). Such a low value (compared to the bulk value of 165 emu.g^{-1}) is due to the surface oxidation of the wires and by the remaining organic matter in the pellet. The density of the pellet, determined using He pycnometry, was found to be $6.76 \pm 0.41 \text{ g.cm}^{-3}$. Taking into account that the organic matter in the particles corresponds to about 7 wt. % and that the CoO layer thickness is 1.2 nm for a nanorod with a mean diameter of 15 nm and a mean length of 130 nm [18], a ratio of 73 wt. % of metallic Co to the total mass of the solid (including CoO and the organic matter) can be estimated. This value is in good agreement with that determined using the apparent M_S value ($113/165 = 68\%$). The temperature dependence of the saturation magnetization is presented on Figure 7a. Two very different behaviours are observed. In the case of Sample (B) (pressed pellet), the saturation magnetization M_S is rather stable up to 550 K; M_S decreases by less than 1% from 300 K to 550 K. At 550 K, a jump of the magnetization is observed corresponding to an increase of 25% with respect to the room temperature magnetization value. At higher temperatures (up to 800 K), the saturation magnetization decreases only moderately (10%). The magnetization jump at 550 K is irreversible and can be explained by the decomposition of remaining metal-organic at the surface of the NRs that reduces the cobalt oxide layer and causes the apparition of added metallic Co. This phenomenon was clearly evidenced by XRD (Figure 4). For the sample (A), the saturation magnetization of the cobalt NRs deposited on an aluminium foil varies only slightly up to 500 K but decreases strongly above this temperature. In this case, the decrease of the magnetization is explained by the oxidation of the cobalt NRs into CoO as was inferred by XRD. The successive washings have removed most of the organic matter (Figure 3) and no reduction can occur. The helium reduced pressure in the oven of the SQUID was not sufficient to prevent the powders from oxidation at high temperature since traces of O_2 were probably present.

The temperature dependence of the coercivities are presented in Figure 7b. When normalized to the to the room temperature coercivity, $H_C(T)/H_C(300K)$, the coercivity of both samples follows the same behaviour over the temperature range 300-500K. The coercivity $\mu_0 H_C$ follows a linear dependence:

$$\frac{\mu_0 H_C}{\mu_0 H_C(300K)} = 1 - a(T - 300)$$

where a is $2.4 \times 10^{-3} \text{ K}^{-1}$. This dependence can be accounted for by the temperature dependence of the magneto-crystalline anisotropy of hcp cobalt. The magneto-crystalline anisotropy of mono-crystalline cobalt is usually described by an anisotropy energy of the form $E_a = K_{u1} \sin^2 \theta + K_{u2} \sin^4 \theta$ with $K_{u1} = 4.1 \times 10^5 \text{ J.m}^{-3}$ and $K_{u2} = 1.4 \times 10^5 \text{ J.m}^{-3}$ at 300 K and is θ

the angle of the magnetization with respect to the c axis. The respective temperature variations of these anisotropy constants is however non-trivial: while the value of K_{u2} monotonously decreases down to $0.4 \times 10^5 \text{ J.m}^{-3}$ at 600K, the value of K_{u1} changes sign at 520 K [22]. The spin reorientation (from parallel to perpendicular to the c -axis) is mainly driven by the change of sign of K_{u1} at 520 K, the effect of K_{u2} being to “smear” the transition so that the reorientation from 0° to 90° takes place over a rather wide temperature range (520-600 K). At 550 K, the spin reorientation is about 40° [23] with a magneto-crystalline energy as low as $0.1 \times 10^5 \text{ J.m}^{-3}$, that is less than a 1/50 of the room temperature anisotropy so that the Co NR can be considered to have no more magneto-crystalline anisotropy.

In the case of sample B, sintering of the wires interferes with the intrinsic magnetic properties of the Co NRs. On the other hand, in the case of sample A, the wires are structurally stable in shape at least up to 600 K and the wires are rather well aligned with a dispersion in their directions smaller than 7° [17]. We can thus consider sample A as consisting of individual particles behaving as Stoner-Wohlfarth particles. At 550K when the magneto-crystalline anisotropy vanishes, the coercivity of elongated ellipsoidal particles with their long axis aligned with the applied field can be expressed as $\mu_0 H_C = 2K_{shape}/M_S$ [24] where K_{shape} corresponds to the effective anisotropy constant related to the shape anisotropy of the particles. Note that this formula is strictly valid only if the magnetization rotation is coherent, which requires that the particle diameter is very small ($\approx 8 \text{ nm}$ for Co). Our NRs dimensions are close to this limit. The value of the coercivity at 550K is $\mu_0 H_C \approx 210 \text{ mT}$ which thus corresponds to the contribution of the shape anisotropy. This represents only half of the theoretical value for an aspect ratio of 5 ($2K_{shape}/M_S \approx 527 \text{ mT}$). The fact that the measured value is significantly smaller than the maximum theoretical value for equivalent ellipsoid can be easily accounted for by the fact that: (i) the NRs assembly is not well aligned which dramatically reduces the coercivity related to the shape anisotropy, (ii) for an equivalent aspect ratio, ellipsoids have a higher coercivity compared to cylinders because of domain nucleation [16] and (iii) we are not working at 0 K so that thermally activated reversal plays a significant role.

From a point of view of using Co NRs as a basis for the fabrication of permanent magnetic materials, one important aspect was to evaluate magnetic dipolar magnetic interactions between nanowires in dense magnetic aggregates. This has been very recently addressed and micromagnetic simulations have shown that dipolar interaction between wires are not detrimental to the high coercivity properties, even for very dense aggregates [17]. With respect to high temperature operation, the present study shows that the temperature dependence of the Co magneto-crystalline anisotropy is a real limitation. K_{MC} not only vanishes around 550 K but becomes negative

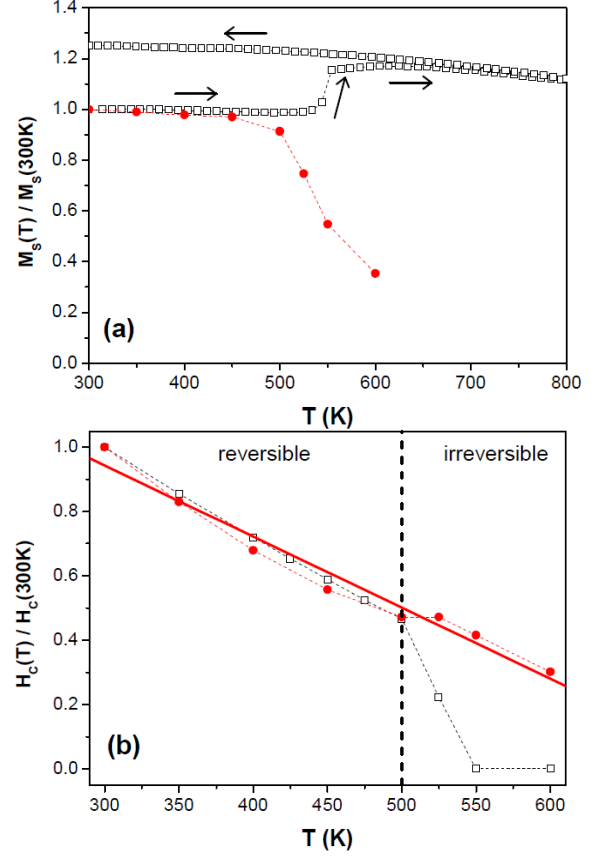


Figure 7: $M_S(T)/M_S(300K)$ (a) and $H_C(T)/H_C(300K)$ (b) as a function of temperature as a function of temperature for sample (A) and sample (B). The solid line is a linear fit to the experimental data corresponding to sample (A), which is given by $\frac{\mu_0 H_C}{\mu_0 H_C(300K)} = 1 - a(T-300)$ (see text for details).

above this temperature, which, as a consequence, leads to magnetic properties which are very sensitive to the temperature. Nevertheless, the materials are rather resilient to high temperatures (up to 550 K) and are competitive with the other existing types of permanent magnetic materials. The magnetic performances of Co nanowires are of the order of $(BH)_{max} \approx 12\text{-}15 \text{ MG Oe}$ at room temperature [12] which rank them in-between ferrites ($\approx 3 \text{ MG Oe}$) and AlNiCo ($\approx 5 \text{ MG Oe}$) and RE-magnets (NdFeB $\approx 40 \text{ MG Oe}$; SmCo $\approx 20\text{-}30 \text{ MG Oe}$). A general drawback of rare earth based materials is their relatively lower Curie temperature (580 K for NdFeB and 1023 K for SmCo) which leads to a significant dependence of the magnetization at high temperatures which is not the case for pure Co systems ($T_C \approx 1300 \text{ K}$). NdFeB magnets cannot be operated at temperatures above 400 K because of irreversible losses. SmCo magnets can be operated at elevated temperatures (up to 523 K typically) which is equivalent to our materials. They have a similar temperature coefficient for the coercive field ($\approx -2 \times 10^{-3} \text{ K}^{-1}$) as Co nanowires.

IV. CONCLUSION

The interest of the Co NRs prepared by the polyol process lies in their well-controlled morphology, diameter smaller than 15 nm, high aspect ratio and shape homogeneity, and, consequently, in their high coercivity at room temperature. In this paper, we have presented a study on structural and magnetic properties of these particles at high temperatures. In the temperature range 300-550 K, we show that the coercivity decreases linearly and that this variation is reversible. This can be accounted for by the temperature dependence of the magneto-crystalline anisotropy of cobalt. At 550 K, 40% of the room temperature coercivity is maintained. This value corresponds to the contribution of the shape anisotropy to the global anisotropy since at 550K the magnetocrystalline contribution has vanished. Above 525 K, the magnetic properties are irreversibly altered either by sintering or by oxidation. In absence of oxygen the decomposition of metal-organic matter remaining at the particle surface reduces the native cobalt oxide layer and provokes coalescence. The coercivity is irreversibly

altered by the loss of shape anisotropy and by the particle growth that may induce a transition from mono- to multi- domains magnetic particles. In slightly oxidative conditions, the growth of a thin oxide layer at the wire surface prevents from sintering but decreases significantly the saturation magnetization. In terms of temperature stability some further work is necessary to prevent both coalescence and oxidation of the wires at high temperatures (>550K). The use of a passivation layer is a possible route to that.

Acknowledgments

The authors gratefully acknowledge the Agence Nationale de la Recherche for their financial support (project 07-NANO-009 MAGAFIL). We thank F. Herbst (ITODYS) for providing the TEM images of nanowires and J.B. Moussy (CEA-IRAMIS) for his help in the magnetometry measurements. The help of Dr. S. Khennache for He pycnometry measurements was greatly appreciated.

-
- [1] Lieber, C. M.; Wang, Z. L.; MRS Bull. 2007, 32, 99.
 - [2] Xia, Y.N.; Yang, P.D.; Sun, Y.G.; Wu, Y.Y.; Mayers, B.; Gates, B.; Yin, Y.D.; Kim, F.; Yan, Y. Q. Adv. Mater. 2003, 15, 353.
 - [3] Sellmyer, D. J.; Zheng, M.; Skomski, R. J. Phys. : Condens. Matter 2001, 13, R433.
 - [4] (a) Tilmaciu, C.M.; Soula, B.; Galibert, A.M.; Lukanov, P. ; Datas, L.; Gonzalez, J.; Barquin, L.F.; Fernandez, J.R.; Gonzalez-Jimenez, F.; Jorge, J.; Flahaut, E. Chem. Commun. 2009, 43, 6664; (b) Weissker, U.; Löffler, M.; Wolny, F.; Lutz, M.U.; Scheerbaum, N.; Klingeler, R.; Gemming, T.; Muhl, T.; Leonhardt, A.; Buchner, B. J. Appl. Phys. 2009, 106, 054909.
 - [5] (a) Campbell, R. ; Bakker, M.G.; Havrilla, G.; Montoya, V.; Kenik, E.A. ; Shamsuzzoha, M. Microporous Mesoporous Mater. 2006, 97, 114; (b) Chernysheva, M.V. ; Sapozhnikova, N.A. ; Eliseev, A.A. ; Lukashin, A.V. ; Tretyakov, Y.D. ; Goernert, P. Pure and Appl.Chem. 2006, 78, 1749; (c) Zhang, Z.; Dai, S.; Blom, D. A.; Shen, J. Chem. Mater. 2002, 14, 965; (d) Luo, H.; Wang, D.; He, J.; Lu, Y. J. Phys. Chem. B 2005, 109, 1919.
 - [6] (a) Vidal, F.; Zheng, Y.; Milano, J.; Demaille, D.; Schio, P.; Fonda, E.; Vodungbo, B. Appl. Phys. Lett. 2009, 95, 152510 ; (b) Schio, P.; Vidal, F.; Zheng, Y.; Milano, J.; Fonda, E.; Demaille, D.; Vodungbo, B.; Varalda, J.; de Oliveira, A. J. A. ; Etgens V. H. Phys. Rev. B 2010, 82, 094436.
 - [7] Li, Y.; Tevaarwerk, E. ; Chang, R.P.H. Chem. Mater. 2006, 18 , 2552.
 - [8] (a) Dumestre, F. ; Chaudret, B. ; Amiens, C. ; Fromen, M.-C. ; Casanove, M.-J. ; Renaud, P. ; Zurcher, P. Angew. Chem. Int. Ed. 2002, 41, 4286. (b) Dumestre, F. ; Chaudret, B. ; Amiens, C. ; Respaud, M. ; Fejes, P. ; Renaud, P. ; Zurcher, P. Angew. Chem. Int. Ed. 2003, 42, 5213.
 - [9] Soumare, Y. ; Piquemal, J.-Y. ; Maurer, T. ; Ott, F. ; Chaboussant, G. ; Falqui, A. ; Viau, G. J. Mater. Chem. 2008, 18, 5696.
 - [10] (a) Y. Xie, J.-M. Zhang, J. Phys. Chem. Sol. 73 (2012) 530-534 ; (b) A. S. Samardak, E. V. Sukovatitsina, A. V. Ognev, L. A. Chebotkevich, R. Mahmoodi, S. M. Peighambari, M. G. Hosseini, F. Nasirpour, J. Phys. : Conf. Ser. 345 (2012) 012011 ; (c) A. Morelos-Gómez, F. López-Uriás, E. Muñoz-Sandoval, C. L. Dennis, R. D. Shull, H. Terrones, M. Terrones, J. Mater. Chem. 20 (2010) 5906-5914 ; (d) X. Huang, L. Li, X. Luo, X. Zhu, G. Li, J. Phys. Chem. C 112 (2008) 1468-1472.
 - [11] O. S. Pak, W. Gao, J. Wang, E. Lauga, Soft Matter 7 (2011) 8169-8181.
 - [12] Maurer, T.; Ott, F. ; Chaboussant, G. ; Soumare, Y.; Piquemal, J.-Y. ; Viau, G. Appl. Phys. Lett. 2007, 91, 172501.
 - [13] Soumare, Y. ; Garcia, C. ; Maurer, T. ; Chaboussant, G. ; Ott, F. ; Fiévet, F. ; Piquemal J.-Y.; Viau, G. Adv. Funct. Mater. 2009, 19, 1971.
 - [14] Soulantica, K.; Wetz, F.; Maynadié, J.; Falqui, A.; Tan, R. P.; Blon, T.; Chaudret, B.; Respaud, M. Appl. Phys. Lett. 2009, 95, 152504.
 - [15] Viau, G.; Garcia, C.; Maurer, T.; Chaboussant, G.; Ott, F.; Soumare, Y.; Piquemal, J.-Y. Phys. Status Solidi A 2009, 206, 663.
 - [16] (14) Ott, F.; Maurer, T.; Chaboussant, G.; Soumare, Y.; Piquemal, J.-Y.; Viau, G. J. Appl. Phys. 2009, 105, 013915.
 - [17] Maurer, T.; Zighem, F.; Fang, W.; Ott, F.; Chaboussant, G.; Soumare, Y.; Ait Atmane, K.; Piquemal, J.-Y.; Viau, G. J. Appl. Phys. 2011, 110, 123924.
 - [18] Maurer, T.; Zighem, F.; Ott, F.; Chaboussant, G.; André, G.; Soumare, Y.; Piquemal, J.-Y.; Viau, G.; Gatel, C. Phys. Rev. B 2009, 80, 064427.

- [19] Karim, S; Toimil-Molares, M.E.; Balogh, A.G.; Ensinger, W.; Cornelius, T.W.; Khan, E.U.; Neumann, R. *Nanotechnology* 2006, 17, 5954
- [20] Nisoli, C.; Abraham, D.; Lookman, T.; Saxena, A. *Phys. Rev. Lett.* 2009, 102, 245504.
- [21] Ciuculescu, D.; Dumestre, F.; Comesaña-Hermo, M.; Chaudret, B.; Spasova, M.; Farle, M.; Amiens, C., *Chem. Mater.* 2009, 21, 3987.
- [22] Ono, F. *J. Phys. Soc. Jap.* 1981, 50, 2564.
- [23] Y. Barnier, R. Pauthenet, G. Rimet, *C. R. Hebd. Acad. Sci.* 253 (1961) 400.
- [24] R. C. O'Handley, *Modern Magnetic Materials, Principles and Applications*, Wiley, New York, 2000, p. 319.